

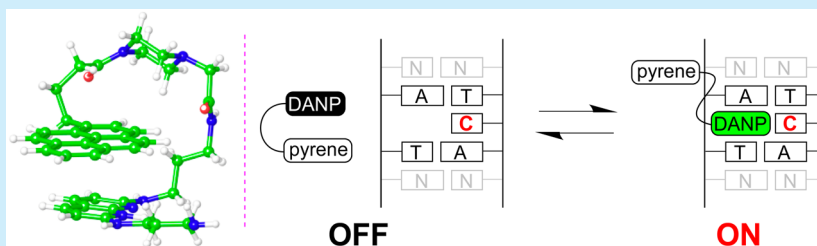
# Synthesis and Photophysical Properties of Fluorescence Molecular Probe for Turn-ON-Type Detection of Cytosine Bulge DNA

Rajiv Kumar Verma,<sup>†</sup> Fumie Takei,<sup>§</sup> and Kazuhiko Nakatani<sup>\*,†</sup>

<sup>†</sup>Department of Regulatory Bioorganic Chemistry, The Institute of Scientific and Industrial Research, Osaka University, Mihogaoka, 8-1, Ibaraki, Osaka 567-0047, Japan

<sup>§</sup>National Defense Medical College, Namiki, 3-2, Tokorozawa, Saitama 359-8513, Japan

**S** Supporting Information



**ABSTRACT:** A fluorescent molecule DANP that binds to cytosine bulge DNA and emits characteristic fluorescence was conjugated to pyrene to give a new fluorescence probe PyDANP. Temperature- and solvent-dependent absorption changes showed that DANP and pyrene chromophores stacked at room temperature in an aqueous buffer solution and quenched fluorescence. Upon binding of DANP moiety in PyDANP to cytosine bulge DNA, the fluorescence from DANP bound to C-bulge increased by ~12-fold, showing that PyDANP is a turn-ON probe for the detection of C-bulge DNA.

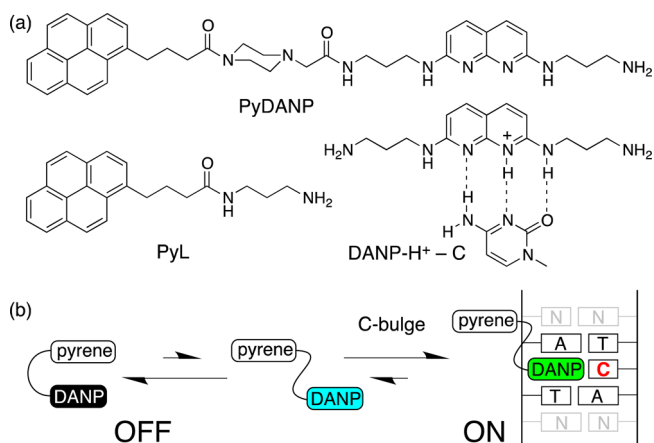
The development of molecular probes that can monitor biochemical processes by interacting with a particular analyte is an important area of research. In recent years, many fluorescent probes have been effectively used to monitor biochemical processes and assays.<sup>1–3</sup> One of the most important bioprobes is the fluorescent molecular probe for selective detection of specific DNA sequences and structures.<sup>4–13</sup> The key for successful design of these fluorescent probes is to maximize the fluorescence change in the absence and presence of the target DNA. Chemistry often used in these molecular probes involves Förster resonance energy transfer<sup>14–18</sup> and photoinduced electron transfer<sup>19–21</sup> because these interactions can be sensitively modulated by the analyte binding. Besides these fluorescent probes using dynamic quenching,<sup>22–25</sup> static quenching was also used for ON-OFF type probes.<sup>26–34</sup>

Static quenching is usually associated with the formation of inter- or intramolecular ground-state complexes<sup>27–29</sup> and can be controlled by electronic properties and spatial orientation of two chromophores.<sup>30–34</sup> Our research group has developed 2,7-diamino-1,8-naphthyridine (DANP) ligand, which binds to cytosine bulge (C-bulge) in duplex DNA upon protonation of a ring nitrogen with concomitant induction of a bathochromic shift of absorption and emission peaks by 30 nm.<sup>35–37</sup> This bathochromic shift enabled us to selectively excite and detect the DANP bound to the C-bulge in the presence of unbound DANP to establish a novel method to monitor the PCR progress.<sup>38–41</sup> The free DANP, however, still absorbs some

energy to give background fluorescence, resulting in lowering the signal to background ratio.

We herein report new fluorescent molecular probe PyDANP (Scheme 1a), where DANP was conjugated with pyrene

**Scheme 1. (a) Structures of PyDANP and DANP with a Hydrogen Bonding Scheme to Cytosine upon Protonation and Reference Compound PyL. (b) Proposed Equilibrium of PyDANP in the OFF State Regarding Fluorescence Emission with the ON State of Complex with C-Bulge DNA**



Received: May 12, 2016

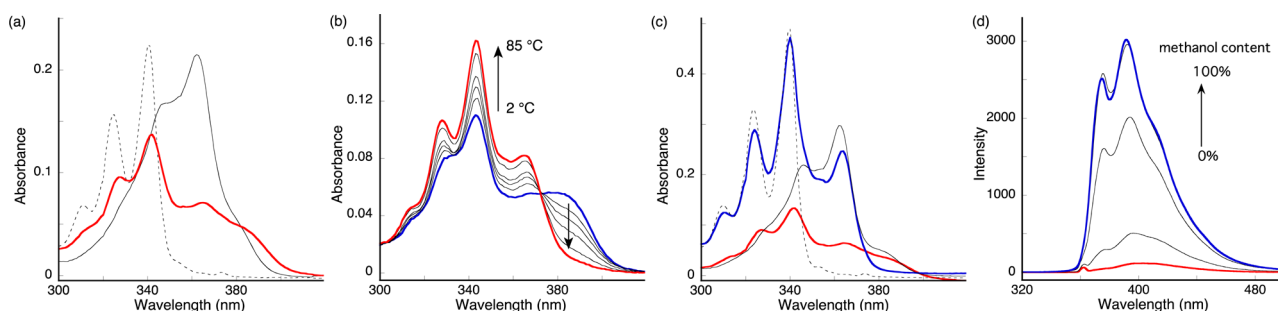


**Figure 1.** (a) UV absorption spectra of 10  $\mu\text{M}$  PyDANP (red line), DANP (black solid line), and PyL (black dotted line) in 10 mM sodium cacodylate buffer (pH 7.0) containing 100 mM sodium chloride at 25  $^{\circ}\text{C}$ . (b) UV absorption spectra of PyDANP with increasing temperature from 2  $^{\circ}\text{C}$  (blue line) to 85  $^{\circ}\text{C}$  (red line). (c) Absorption spectra of ligands (10  $\mu\text{M}$ ) in methanol (PyDANP, blue line; PyL, black dotted line; DANP, black line) with comparison of spectra of PyDANP in an aqueous buffer solution (red line) at 25  $^{\circ}\text{C}$ . (d) Fluorescence spectra of PyDANP with various methanol contents: 0 (red), 25, 50, 75, and 100% (blue) at 25  $^{\circ}\text{C}$ . Excitation wavelength is 365 nm, which is characteristic of a free DANP moiety.

(Figure S1 and S2). Covalent attachment of two chromophores increases the probability of intramolecular stacking interaction in aqueous environment, and we could anticipate that the fluorescence of both chromophores would be suppressed by static quenching (Scheme 1b). As a counterpart to DANP chromophore pyrene was selected because of wide aromatic surface facilitating the molecular stacking. Among several linkers we examined, the linker containing piperazine showed the most effective ON–OFF properties. In addition to primary amine and the 2,7-diaminonaphthyridine moiety, one of the nitrogens in piperazine remained basic and protonated at neutral pH, making PyDANP quite soluble in aqueous buffer solution. On the basis of this molecular design, the equilibrium of DANP stacking with pyrene could be modulated by the presence of C-bulge DNA. This would drive the equilibrium toward the DANP–C-bulge complex to release DANP from stacking with pyrene and emit characteristic fluorescence. In fact, fluorescence of PyDANP was kept at a low level in the absence of C-bulge and increased by 12-fold in the presence of C-bulge DNA with A–T flanking base pairs.

Absorption and fluorescence spectra of PyDANP and reference compounds DANP and PyL were measured in the buffer solution. While PyL and DANP showed defined peaks in the absorption spectra at 340 and 362 nm, respectively, PyDANP showed a peak at 343 nm and unstructured broad peaks at  $\sim 380$  nm (Figure 1a). The absorption spectrum of PyDANP is not the sum of absorption spectra of PyL and DANP, indicating the electronic interaction between two chromophores in PyDANP. Since the electronic perturbations were speculated due to the stacking interaction of two chromophores, we then measured absorption spectra of PyDANP at different temperatures (Figure 1b). As the temperature increased from 2 to 85  $^{\circ}\text{C}$ , marked changes in the absorption spectra involving the isosbestic point were observed. The broad absorption peak at  $\sim 380$  nm observed at 2  $^{\circ}\text{C}$  kept decreasing in absorption as the temperature increased. These spectral changes were reversible (Figure S3). These changes suggested the possibility of existence of intramolecular folded structure, which can be easily disrupted at higher temperature. To gain further insight into molecular interactions which lead to the origin of broad absorption bands at  $\sim 380$  nm, we investigated the nature of absorption in organic solvent (Figure 1c). The absorption spectrum of PyDANP in methanol showed distinct peaks at 340 and 365 nm, which corresponded well to the peaks observed for PyL and DANP in methanol,

respectively (Figure S4). In contrast, the broad peak at 380 nm was not detected for PyDANP spectra in methanol.

The fluorescence of PyDANP was measured in a buffer solution with various methanol contents (Figure 1d). In the aqueous buffer solution, the fluorescence of PyDANP was low in intensity (fluorescence quantum yield  $\Phi_{\text{F}}$  0.02), although both PyL and DANP emit intense fluorescence under the same conditions (Figure S5). As the content of methanol increased, the fluorescence of PyDANP increased. With 75% methanol in the buffer solution, the fluorescence spectrum was almost superimposable with the fluorescence spectrum in methanol. Hydrophobic forces are not effective in methanol, and we could observe the fluorescence from both pyrene and DANP moieties of PyDANP. Linear correlation of absorbance and fluorescence intensity of PyDANP with the ligand concentration up to 80  $\mu\text{M}$  excluded the possibility of intermolecular aggregation (Figure S6 and S7). Components of PyDANP (PyL, DANP, and a mixture of PyL and DANP) also did not show any significant shape and structural changes in absorption and fluorescence spectra with increasing concentrations (Figures S8–S10). Both temperature- and solvent-dependent absorption and fluorescence changes observed for PyDANP suggested that pyrene and DANP chromophores in PyDANP produced a stacked complex in the aqueous buffer solution, where the fluorescence of PyDANP was kept in a low intensity.

Cold spray ionization time-of-flight mass spectrometry (CSI-TOF-MS) analysis of PyDANP binding to C-bulge DNA firmly confirmed the formation of the 1:1 complex (Figure 2). The hairpin DNA having C-bulge in the TCA/T<sub>A</sub> sequence (10  $\mu\text{M}$ ) showed  $[\text{TCA/T}_A]^{5-}$  and  $[\text{TCA/T}_A]^{6-}$  ions under the conditions, and these ions decreased in intensity in the presence of PyDANP (20  $\mu\text{M}$ ) with concomitant increase of ions corresponding to  $[\text{TCA/T}_A+\text{PyDANP}]^{5-}$  and  $[\text{TCA/T}_A+\text{PyDANP}]^{6-}$ , showing the formation of the 1:1 complex of C-bulge DNA and PyDANP.

Having confirmed that PyDANP showed weak fluorescence in aqueous buffer solution at room temperature and that PyDANP produces a 1:1 complex with C-bulge hairpin DNA, we then investigated the equilibrium toward the bound state which may be driven by the C-bulge hairpin DNA and may result in the emission of characteristic fluorescence from the DANP–C-bulge complex (Scheme 1b). The absorption spectrum of PyDANP with DNA containing C-bulge flanked by TA/AT base pairs (TCA/T<sub>A</sub>) showed a bathochromic shift in the peak at 342 to 350 nm and the unstructured peak at 380 to 390 nm with increased absorbance (Figure 3a).

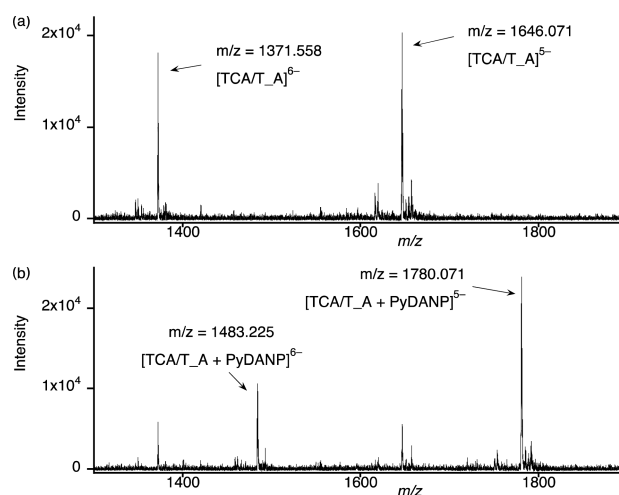


**Figure 2.** CSI-TOF-MS spectra of (a) C-bulge hairpin DNA TCA/T\_A and (b) TCA/T\_A with PyDANP. Solution conditions: 1:1 aqueous solution of methanol containing 50 mM ammonium acetate with 10  $\mu$ M DNA and 20  $\mu$ M PyDANP solution. TCA/T\_A: 5'-GTCA TCA ACAACTTTTGTGTTATGAC-3'. Bulge site is shown in bold type.

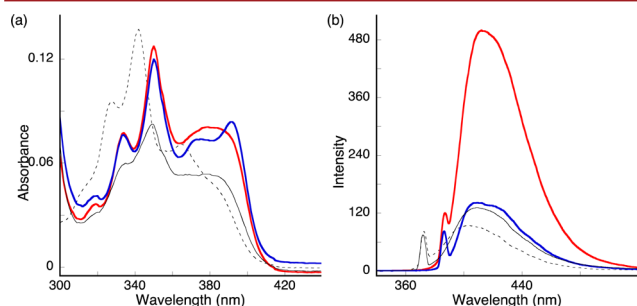


**Figure 3.** (a) Absorption and (b) emission spectra of PyDANP (10  $\mu$ M) (dotted line) in the presence of DNA (10  $\mu$ M). Key: C-bulge TCA/T\_A (red); C-bulge GCG/C\_C (blue); full match dsDNA (black). Solution conditions: 10 mM sodium cacodylate buffer (pH 7.0) containing 100 mM sodium chloride 25  $^{\circ}$ C. Excitation wavelength was 375 and 390 nm in the absence and presence of DNA, respectively. GCG/C\_C: 5'-GTCAGCGACAACCTTTTGTGTCCTGAC-3'; FM: 5'-GTCAGCGACAACCTTTTGTGTCCTGAC-3'. Bulge site is shown in bold type.

Similar spectral changes were also observed for the DNA containing C-bulge flanked by GC/GC base pairs (GCG/C\_C). With the fully matched double-stranded DNA (GC/GC), we observed peak shift at 342 nm, but the peak shift at 380 nm was not significant. The shift in absorption maxima at 350 nm might be attributed to pyrene interaction with DNA (Figure S11). The fluorescence spectrum of PyDANP was most apparent with the TCA/T\_A DNA to show fluorescence at 410 nm with increased intensity ( $\Phi_F$  0.17) (Figure 3b). This emission peak shows approximately 20 nm bathochromic shift from that of PyDANP alone, confirming that the emission is from the DANP–C-bulge complex (cf. DANP fluorescence spectra in Figure S5). In contrast, a marked increase of fluorescence intensity was not observed with GCG/C\_C DNA ( $\Phi_F$  0.04), although the absorption change was most significant. This is likely because G–C base pairs flanking the C-bulge facilitate the DANP binding by the stacking stabilization in the C-bulge–DANP complex, but G–C base pairs simultaneously quench the fluorescence from the neighboring DANP–C-bulge

complex.<sup>36</sup> The presence of fully matched DNA did not increase the fluorescence intensity ( $\Phi_F$  0.06), further confirming that the increased fluorescence at 410 nm was in fact the result of DANP binding to the C-bulge in the TCA/T\_A sequence.

Finally, we compared the relative fluorescence change of PyDANP upon binding to C-bulge hairpin DNA in the TCA/T\_A sequence with that observed for the parent molecule DANP (Figure 4). Both PyDANP and DANP were excited at

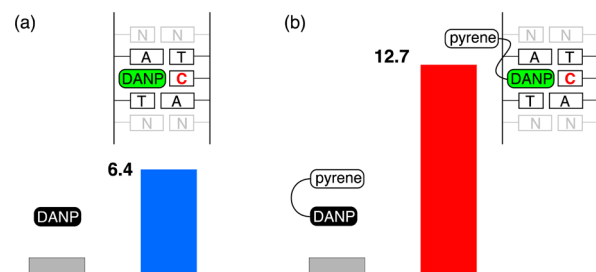


**Figure 4.** Relative fluorescence change for a) DANP (10  $\mu$ M) and b) PyDANP (10  $\mu$ M) upon binding with TCA/T\_A DNA (20  $\mu$ M). All solution were prepared in 10 mM sodium cacodylate buffer (pH 7.0) containing 100 mM sodium chloride 25  $^{\circ}$ C. Excitation wavelength was fixed at 390 nm, which is characteristic for DANP bound to cytosine..

the same wavelength of 390 nm regardless of the absence and presence of C-bulge hairpin DNA. The fold increase of fluorescence at 410 nm observed for PyDANP in the presence of C-bulge DNA was about 12.7, whereas it was 6.4 for DANP. This is due to the decreased fluorescence intensity of the unbound state of PyDANP by the static quenching with pyrene as compared to that state of DANP.

In conclusion, the new ligand PyDANP showed  $\sim$ 12-fold increase in fluorescence intensity in the presence of a C-bulge hairpin DNA with the TCA/T\_A sequence. Temperature- and solvent-dependent changes in the absorption spectra suggested the intramolecular stacking of DANP moiety with pyrene, resulting in a fluorescence quenching. The intramolecular stacking state of PyDANP causing quenching of DANP fluorescence was in equilibrium with DANP-bound state with the C-bulge, resulting in emission of DANP fluorescence by cancelling pyrene stacking. These results demonstrated that PyDANP could be used as a turn-ON probe for the detection of C-bulge DNA with higher signal to background ratio than the parent molecule DANP shows. Further studies on the potential application of PyDANP are now underway in these laboratories.

## ■ ASSOCIATED CONTENT

### Supporting Information

The Supporting Information is available free of charge on the ACS Publications website at DOI: 10.1021/acs.orglett.6b01378.

Synthetic scheme and compound characterization data for ligand PyDANP; additional UV and fluorescence data for clarification of discussions (PDF)

## ■ AUTHOR INFORMATION

### Corresponding Author

\*E-mail: nakatani@sanken.osaka-u.ac.jp.

## Notes

The authors declare no competing financial interest.

## ACKNOWLEDGMENTS

This work was supported by JSPS KAKENHI Grant-in-Aid for Specially Promoted Research (26000007). R.K.V. acknowledges JSPS for a postdoctoral fellowship for foreign researchers (No. P14039). This research is also partially supported by the Platform Project for Supporting Drug Discovery and Life Science Research (Platform for Drug Discovery, Informatics and Structural Life Science) from the Ministry of Education, Culture, Sports, Science and Technology (MEXT).

## REFERENCES

- (1) Lakowicz, J. R. *Principles of Fluorescence Spectroscopy*, 3rd ed.; Springer: New York, 2006.
- (2) Valeur, B.; Berberan-Santos, M. N. *Molecular Fluorescence: Principles and Applications*, 2nd ed.; Wiley-VCH: Weinheim, 2013.
- (3) de Silva, A. P.; Gunaratne, H. Q.; Gunnlaugsson, T.; Huxley, A. J. M.; McCoy, C. P.; Rademacher, J. T.; Rice, T. E. *Chem. Rev.* **1997**, *97*, 1515–1566 and references cited therein.
- (4) Juskowiak, B. *Anal. Bioanal. Chem.* **2011**, *399*, 3157–3176.
- (5) (a) Kim, K. T.; Heo, W.; Joo, T.; Kim, B. H. *Org. Biomol. Chem.* **2015**, *13*, 8470–8478. (b) Venkatesan, N.; Seo, Y. J.; Kim, B. H. *Chem. Soc. Rev.* **2008**, *37*, 648–663.
- (6) (a) Michaelis, J.; van der Heden van Noort, G. J.; Seitz, O. *Bioconjugate Chem.* **2014**, *25*, 18–23. (b) Kohler, O.; Jarikote, D. V.; Seitz, O. *ChemBioChem* **2005**, *6*, 69–77.
- (7) (a) Li, S.; Langenegger, S. M.; Häner, R. *Chem. Commun.* **2013**, *49*, 5835–5837. (b) Malinovsky, V. L.; Wenger, D.; Häner, R. *Chem. Soc. Rev.* **2010**, *39*, 410–422.
- (8) (a) McCoy, L. S.; Shin, D.; Tor, Y. *J. Am. Chem. Soc.* **2014**, *136*, 15176–15184. (b) Sinkeldam, R. W.; Greco, N. J.; Tor, Y. *Chem. Rev.* **2010**, *110*, 2579–2619.
- (9) (a) Saito, Y.; Suzuki, A.; Yamauchi, T.; Saito, I. *Tetrahedron Lett.* **2015**, *56*, 3034–3038. (b) Okamoto, A.; Saito, Y.; Saito, I. *J. Photochem. Photobiol., C* **2005**, *6*, 108–122.
- (10) (a) Holzhauser, C.; Wagenknecht, H.-A. *J. Org. Chem.* **2013**, *78*, 7373–7379. (b) Ensslen, P.; Wagenknecht, H.-A. *Acc. Chem. Res.* **2015**, *48*, 2724–2733.
- (11) (a) Takada, T.; Yamaguchi, K.; Tsukamoto, S.; Nakamura, M.; Yamana, K. *Analyst* **2014**, *139*, 4016–4021. (b) Takada, T.; Takemura, M.; Kawano, Y.; Nakamura, M.; Yamana, K. *Langmuir* **2015**, *31*, 3993–3998.
- (12) (a) Dziuba, D.; Jurkiewicz, P.; Cebecauer, M.; Hof, M.; Hocek, M. *Angew. Chem., Int. Ed.* **2016**, *55*, 174–178. (b) Hocek, M. *J. Org. Chem.* **2014**, *79*, 9914–9921.
- (13) Okamoto, A. *Chem. Soc. Rev.* **2011**, *40*, 5815–5828.
- (14) Hussain, S. A.; Dey, D.; Chakraborty, S.; Saha, J.; Roy, A. D.; Chakraborty, S.; Debnath, P.; Bhattacharjee, D. *Sci. Lett. J.* **2015**, *4*, 119/1–119/16 and references cited therein.
- (15) Lee, L. G.; Connell, C. R.; Bloch, W. *Nucleic Acids Res.* **1993**, *21*, 3761–3766.
- (16) Hillisch, A.; Lorenz, M.; Diekmann, S. *Curr. Opin. Struct. Biol.* **2001**, *11*, 201–207.
- (17) Jares-Erijman, E. A.; Jovin, T. M. *Nat. Biotechnol.* **2003**, *21*, 1387–1395 and references cited therein.
- (18) Lee, H. N.; Xu, Z.; Kim, S. K.; Swamy, K. M. K.; Kim, Y.; Kim, S.-J.; Yoon, J. *J. Am. Chem. Soc.* **2007**, *129*, 3828–3829.
- (19) de Silva, A. P.; Moody, T. S.; Wright, G. D. *Analyst* **2009**, *134*, 2385–2393 and references cited therein.
- (20) Zhang, W.; Ma, Z.; Du, L.; Li, M. *Analyst* **2014**, *139*, 2641–2649.
- (21) Hama, Y.; Urano, Y.; Koyama, Y.; Kamiya, M.; Bernardo, M.; Paik, R. S.; Shin, I. S.; Paik, C. H.; Choyke, P. L.; Kobayashi, H. *Cancer Res.* **2007**, *67*, 2791–2799.
- (22) Chen, Y.; Tsao, K.; Keillor, J. W. *Can. J. Chem.* **2015**, *93*, 389–398.
- (23) Marras, S. A. E. *Mol. Biotechnol.* **2008**, *38*, 247–255.
- (24) Tyagi, S.; Bratu, D. P.; Kramer, F. R. *Nat. Biotechnol.* **1998**, *16*, 49–53.
- (25) Wang, K.; Tang, Z.; Yang, C. J.; Kim, Y.; Fang, X.; Li, W.; Wu, Y.; Medley, C. D.; Cao, Z.; Li, J.; Colon, P.; Lin, H.; Tan, W. *Angew. Chem., Int. Ed.* **2009**, *48*, 856–870.
- (26) Bernacchi, S.; Mely, Y. *Nucleic Acids Res.* **2001**, *29*, e62/1–e62/8.
- (27) Khairutdinov, R. F.; Serpone, N. *J. Phys. Chem. B* **1997**, *101*, 2602–2610.
- (28) Arbeloa, I. L. *J. Chem. Soc., Faraday Trans. 2* **1981**, *77*, 1725–1733.
- (29) West, W.; Pearce, S. *J. Phys. Chem.* **1965**, *69*, 1894–1903.
- (30) Johansson, M. K.; Fidler, H.; Dick, D.; Cook, R. M. *J. Am. Chem. Soc.* **2002**, *124*, 6950–6956.
- (31) Johansson, M. K.; Cook, R. M. *Chem. - Eur. J.* **2003**, *9*, 3466–3471.
- (32) Hirano, H.; Akiyama, J.; Mori, S.; Kagechika, H. *Org. Biomol. Chem.* **2010**, *8*, 5568–5575.
- (33) (a) Sato, T.; Sato, Y.; Iwai, K.; Kuge, S.; Nishizawa, S.; Teramae, N. *Chem. Commun.* **2015**, *51*, 1421–1424. (b) Nishizawa, S.; Sato, Y.; Xu, Z.; Morita, K.; Li, M.; Teramae, N. *Supramol. Chem.* **2010**, *22*, 467–476.
- (34) (a) Hori, Y.; Ueno, H.; Mizukami, S.; Kikuchi, K. *J. Am. Chem. Soc.* **2009**, *131*, 16610–16611. (b) Minoshima, M.; Matsumoto, T.; Kikuchi, K. *Anal. Chem.* **2014**, *86*, 7925–7930.
- (35) Suda, H.; Kobori, A.; Zhang, J.; Hayashi, G.; Nakatani, K. *Bioorg. Med. Chem.* **2005**, *13*, 4507–4512.
- (36) Takei, F.; Suda, H.; Hagihara, M.; Zhang, J.; Kobori, A.; Nakatani, K. *Chem. - Eur. J.* **2007**, *13*, 4452–4457.
- (37) Zhang, J.; Takei, F.; Nakatani, K. *Bioorg. Med. Chem.* **2007**, *15*, 4813–4817.
- (38) Takei, F.; Igarashi, M.; Hagihara, H.; Oka, Y.; Soya, Y.; Nakatani, K. *Angew. Chem., Int. Ed.* **2009**, *48*, 7822–7824.
- (39) Takei, F.; Tani, H.; Matsuura, Y.; Nakatani, K. *Bioorg. Med. Chem. Lett.* **2014**, *24*, 394–396.
- (40) Takei, F.; Igarashi, M.; Oka, Y.; Koga, Y.; Nakatani, K. *ChemBioChem* **2012**, *13*, 1409–1412.
- (41) Chen, H.; Takei, F.; Koay, E. S.-C.; Nakatani, K.; Chu, J. J. H. *J. Mol. Diagn.* **2013**, *15*, 227–233.